

# Design, Synthesis, and Circular Dichroism Investigation of a Peptide-Sandwiched MesoHEME

David R. Benson,<sup>\*,†</sup> Bradley R. Hart,<sup>†</sup> Xiao Zhu,<sup>†</sup> and Michael B. Doughty<sup>‡</sup>

Contribution from the Departments of Chemistry and Medicinal Chemistry, The University of Kansas, Lawrence, Kansas 66045-0046

Received February 15, 1995<sup>⊗</sup>

**Abstract:** Two identical 13 residue peptides (**2**) have been covalently linked to iron(III) mesoporphyrin IX via amide formation between the heme propionyl groups and the  $\epsilon$ -amine of lysine side chains. The peptide was designed such that coordination of the imidazolyl side chain of the histidine residue in each peptide to the heme metal would lead to helix induction. The resulting peptide-sandwiched mesoheme (**1**) exists as a pair of interconvertible diastereomers due to the substitution pattern of the heme moiety. Bisimidazole coordination of the iron in **1** is demonstrated by ultraviolet/visible (UV/vis) spectroscopy. Circular dichroism (CD) experiments in the far UV (190–240 nm) reveal that in aqueous solution at 8 °C the peptides in **1** are approximately 52%  $\alpha$ -helical and that helicity can be increased to a maximum measured value of 97% by the addition of 2,2,2-trifluoroethanol (TFE) and other cosolvents. Features arising from the heme moiety are observed in CD spectra, including the Soret and  $\alpha$  and  $\beta$  bands. We provide evidence that the heme contributes positive ellipticity to the far-UV CD spectrum, complicating quantitation of peptide helicity based on the mean residue ellipticity at 220 nm ( $\theta_{220}$ ). The molar ellipticity at  $\lambda_{\max}$  of the CD Soret band ( $\theta_{m403}$ ) is a function of peptide conformation, changing markedly upon addition of cosolvents and with increases in temperature. The spectral changes likely result from a reorientation of the peptide backbone amides relative to the  $B_x$  and  $B_y$  electronic transitions of the heme. A chromophore-bearing analogue of the peptide used in the synthesis of **1** (**6**) exists in a random coil conformation in aqueous solution, exhibiting no innate helical tendencies. Helicity of **6** reaches 80% in 50 volume % TFE, but helicity can be increased even further by using the more acidic solvent 1,1,1,3,3,3-hexafluoro-2-propanol (HFIP). A mixture of diastereomeric mono-peptide adducts formed from **1** and **6** (**3a,b**) has also been isolated and is found to have strong concentration-dependent behavior. UV/vis suggests that these phenomena can be attributed to aggregation, which is a consequence of **3a,b** having one face of the heme exposed to the solvent.

## Introduction

In an effort to understand the forces involved in protein folding and stability, much effort has been directed toward the design of monomeric peptides which favor  $\alpha$ -helical conformations in aqueous solution.<sup>1</sup> Baldwin and co-workers discovered that short alanine-based peptides are highly helical in water near 0 °C.<sup>1–4</sup> These have their natural counterparts in the anti-freeze polypeptides of arctic fishes.<sup>5</sup> Amino acids with aromatic or  $\beta$ -branched side chains, however, act as helix-breakers in monomeric peptides due to constraints on side chain rotational entropy when in an  $\alpha$ -helical conformation.<sup>6</sup>

Several recent reports have described helix-induction in structurally diverse polypeptides by specifically engineered side

chain-side chain interactions.<sup>7,8</sup> We have extended this strategy to the design of a water soluble model hemoprotein, peptide-sandwiched mesoheme (**1**), in which folding of two identical peptides (**2**) from completely random coil conformations into structures with approximately 52% helical content results from histidine to iron bonding with a covalently attached iron(III) mesoporphyrin IX moiety.

Model hemoproteins composed of heme-peptide adducts have been prepared and studied as water soluble oxidation catalysts,<sup>9</sup> as templates for the study of long-range electron transfer,<sup>10</sup> and as novel membrane-spanning proteins.<sup>11</sup> In those

<sup>†</sup> Department of Chemistry.

<sup>‡</sup> Department of Medicinal Chemistry.

<sup>⊗</sup> Abstract published in *Advance ACS Abstracts*, August 1, 1995.

(1) Reviewed in: Scholtz, J. M.; Baldwin, R. L. *Annu. Rev. Biophys. Biomol. Struct.* **1992**, *21*, 95–118.

(2) Convincing experimental evidence has surfaced suggesting that certain alanine-based peptides, form  $3_{10}$  helices in water.<sup>3</sup> Theoretical studies indicate, however, that  $\alpha$ -helices are significantly more stable than  $3_{10}$  helices in alanine-based peptides.<sup>4</sup>

(3) (a) Miick, S. M.; Martinez, G. V.; Fiori, W. R.; Todd, A. P.; Millhauser, G. L. *Nature* **1992**, *359*, 653–655. (b) Fiori, W. R.; Miick, S. M.; Millhauser, G. L. *Biochemistry* **1993**, *32*, 11957–11962.

(4) (a) Tirado-Rives, J.; Maxwell, D. S.; Jorgensen, W. L. *J. Am. Chem. Soc.* **1993**, *115*, 11590–11593. (b) Smythe, M. L.; Huston, S. E.; Marshall, G. R. *J. Am. Chem. Soc.* **1993**, *115*, 11594–11595.

(5) Yang, D. S. C.; Sax, M.; Chakrabarty, A.; Hew, C. L. *Nature* **1988**, *333*, 232–237.

(6) (a) Padmanabhan, S.; Marqusee, S.; Ridgeway, T.; Laue, T. M.; Baldwin, R. L. *Nature (London)* **1990**, *34*, 268–270. (b) Merutka, G.; Lipton, W.; Shalongo, W.; Park, S.-H.; Stellwagen, E. *Biochemistry* **1990**, *29*, 7511–7515. (c) Piela, L.; Nemethy, G.; Scheraga, H. A. *Biopolymers* **1987**, *26*, 1273–1286.

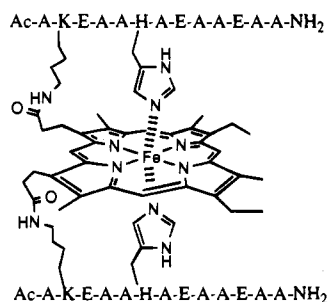
(7) Covalent: (a) Jackson, D. Y.; King, D. S.; Chmielewski, J.; Singh, S.; Schultz, P. G. *J. Am. Chem. Soc.* **1991**, *113*, 9391–9392. (b) Chorev, M.; Roubini, E.; McKee, R. L.; Gibbons, S. W.; Goldman, M. E.; Caulfield, M. P.; Rosenblatt, M. *Biochemistry* **1991**, *30*, 5968–5974. (c) Zhou, H. X.; Hull, L. A.; Kallenbach, N. R.; Mayne, L.; Bai, Y.; Englander, S. W. *J. Am. Chem. Soc.* **1994**, *116*, 6482–6483.

(8) Metal-ligand: (a) Ghadiri, M. R.; Choi, C. J. *J. Am. Chem. Soc.* **1990**, *112*, 1630–1632. (b) Ghadiri, M. R.; Fernholz, A. K. *J. Am. Chem. Soc.* **1990**, *112*, 9633–9635. (c) Ruan, F.; Chen, Y.; Hopkins, P. B. *J. Am. Chem. Soc.* **1990**, *112*, 9403–9404.

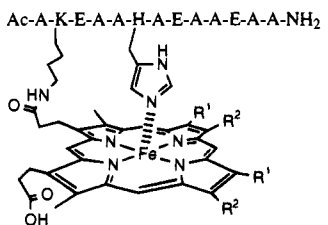
(9) (a) Sasaki, T.; Kaiser, E. T. *Biopolymers* **1990**, *29*, 79–88. (b) Casella, L.; Gullotti, M.; De Gioia, L.; Monzani, E.; Chillemi, F. *J. Chem. Soc. Dalton Trans.* **1991**, 2945–2953. (c) Adams, P. A.; Goold, R. D. *J. Chem. Soc. Chem. Commun.* **1990**, 97–98 and references therein.

(10) (a) Choma, C. T.; Lear, J. D.; Nelson, M. J.; Dutton, P. L.; Robertson, D. E.; DeGrado, W. F. *J. Am. Chem. Soc.* **1994**, *116*, 856–865. (b) Robertson, D. E.; Farid, R. S.; Moser, C. C.; Urbauer, J. L.; Mulholland, S. E.; Pidikiti, R.; Lear, J. D.; Wand, A. J.; DeGrado, W. F.; Dutton, P. L. *Nature (London)* **1994**, *368*, 425–432.

(11) (a) Akerfeldt, K. S.; Kim, R. M.; Camac, D.; Groves, J. T.; Lear, J. D.; DeGrado, W. F. *J. Am. Chem. Soc.* **1992**, *114*, 9656–9657. (b) Mihara, H.; Nishino, N.; Hasegawa, R.; Fujimoto, T. *Chem. Lett.* **1992**, 1805–1808. (c) Nishino, N.; Mihara, H.; Kiyota, H.; Kobata, K.; Fujimoto, T. *J. Chem. Soc., Chem. Commun.* **1993**, 162–163.



1

3a: R<sup>1</sup> = Me; R<sup>2</sup> = Et3b: R<sup>1</sup> = Et; R<sup>2</sup> = MeAc-A-K-E-A-A-H-A-E-A-A-E-A-A-NH<sub>2</sub> (2)

model hemoproteins containing  $\alpha$ -helical peptides,<sup>9a,10,11</sup> the helicity arises as a result of intramolecular peptide-peptide association, not from metal to ligand coordination. Some early hemoprotein model compounds included intramolecular coordination between the heme metal and an amino acid side chain (e.g., histidine, cysteine) or a similar group linked by a tether to the heme, in an attempt to recreate the ligand environment of the natural protein system.<sup>12</sup> However, these compounds were generally designed for solubility in organic solvents. The water-soluble peptide-sandwiched mesoheme **1** illustrates beautifully how metal to ligand bond formation can determine the structure of a short peptide having a low helical propensity and as such serves as a new concept for hemoprotein design.

Heme features in CD spectra of hemoproteins<sup>13</sup> and of heme-peptide adducts<sup>14</sup> have been observed in many instances, most notably in the Soret region. Although a common phenomenon, the interactions which determine the nature of the heme CD features are still the subject of ongoing investigations.<sup>15</sup> A CD Soret band having a negative Cotton effect is observed for **1**, its intensity decreasing as the helical content of the peptides increases in the presence of alcoholic cosolvents. Reduced peptide helicity resulting from an increase in temperature also causes a decreased Soret spectrum. We hypothesize that the decrease in the CD Soret band arises via changes in the nature of the interactions between the peptide and the heme as the peptide conformation is altered. The important interactions are likely between the B<sub>x</sub> and B<sub>y</sub> ( $\pi$ - $\pi^*$ ) transitions of the heme and transition dipoles of the peptide backbone amides.<sup>15</sup> We

(12) Reviewed in Morgan, B.; Dolphin, D. *Struct. Bonding (Berlin)* **1987**, *64*, 115–203.

(13) Hemoprotein CD: (a) Nicola, N. A.; Minasian, E.; Appleby, C. A.; Leach, S. J. *Biochemistry* **1975**, *14*, 5141–5149. (b) Zand, R.; Vinogradov, S. *Biochem. Biophys. Res. Commun.* **1967**, *26*, 121–127. (c) Sugita, Y.; Dohi, Y.; Yoneyama, Y. *Biochem. Biophys. Res. Commun.* **1968**, *31*, 447–452. (d) Gersonde, K.; Sick, H.; Wollmer, A.; Buse, G. *Eur. J. Biochem.* **1972**, *25*, 181–189. (e) Shikama, K.; Suzuki, T.; Sugawara, Y.; Katagiri, T.; Takage, T.; Hatano, M. *Bioch. Biophys. Acta* **1982**, *701*, 138–141.

(14) Heme-peptide adduct CD: (a) Urry, D. W. *J. Biol. Chem.* **1967**, *242*, 4441–4448. (b) Urry, D. W. *J. Am. Chem. Soc.* **1967**, *89*, 4190–4196. (c) Urry, D. W.; Pettegrew, J. W. *J. Am. Chem. Soc.* **1967**, *89*, 5276–5283. (d) Okuyama, K.; Murakami, T.; Nozawa, T.; Hatano, M. *Chem. Lett.* **1982**, 111–114.

(15) Mizutani, T.; Ema, T.; Yoshida, T.; Renne, T.; Ogoshi, H. *Inorg. Chem.* **1994**, *33*, 3558–3566.

also provide evidence that the heme contributes positive ellipticity in far-UV CD spectra of **1**, resulting in underestimation of peptide helical content, although the effect cannot be quantitated. Peptide-sandwiched mesoheme **1** thus represents a conformationally flexible system which allows us to more thoroughly investigate the CD features which arise from the heme moiety than has been possible with previous hemoprotein model compounds.

## Experimental Section

**General Methods.** All reagents were of commercial grade and were used without further purification except for the following. Pyridine was distilled from KOH prior to use, and dimethyl sulfoxide (DMSO) was dried over 4 Å molecular sieves. Amino acids and resins were purchased from Advanced Chemtech (Louisville, KY) except for *N*- $\alpha$ -t-BOC-*N*- $\epsilon$ -(2-chloro-CBZ)-L-lysine (Fisher Biotech) and *N*-Fmoc- $\epsilon$ -aminocaproic acid (Bachem California). Peptide **2** was synthesized on a Vega Biotechnologies Coupler 1000 peptide synthesizer using *t*-BOC chemistry on MBHA resin (100–200 mesh, 1% DVB, substitution level 0.53 mmol/g). Deprotection and cleavage from the resin was performed by Immuno-Dynamics Corp. in San Diego, CA. The peptide was purified by HPLC (Rainin system HPLX) on a 2.2 cm Vydac C18 peptide/protein column using a gradient of acetonitrile in 0.1% TFA (5% to 40% over 40 min) at a flow rate of 8 mL/min. Amino acid analysis: AA, found (calc); A, 1.00 (1); E, 3.06 (3); H, 0.98 (1); K, 0.96 (1). Peptide **5** was prepared on a Rainin PS3 automated synthesizer using Fmoc chemistry on Rink resin (100–200 mesh, 1% DVB, substitution level 0.56 mmol/g), followed by deprotection and cleavage from the resin using Reagent K.<sup>16</sup> HPLC purification was achieved by the same method recorded for **2**. Amino acid analysis: AA, found (calc);  $\epsilon$ -aminocaproic acid, present (1); A, 7.81 (8); E, 3.15 (3); H, 1.03 (1); K, 1.01 (1). Both peptides were homogeneous as determined by analytical HPLC and by fast atom bombardment mass spectrometry (FAB-MS). FAB-MS measurements were made on a VG AutoSpec with high resolution double sector. Amino acid analyses were performed by the KU Biochemical Research Services Laboratory using FITC precolumn derivatization of peptides hydrolyzed in 6 M HCl (0.01% phenol) for 24 h.

Mesoporphyrin IX (Aldrich) was converted to the ferric complex by refluxing with excess Fe(OAc)<sub>2</sub> in acetic acid.<sup>17</sup> The bis(*p*-nitrophenyl) ester of iron(III) mesoporphyrin IX (**4**) was subsequently prepared using the method of Collman et al.<sup>18</sup>

Ultraviolet/visible (UV/vis) spectra were recorded on a Shimadzu UV-2100 recording spectrophotometer, using a CPS cell positioner with electronic temperature control. Temperature within the cell was measured using an Omega Model HH200 thermometer with a K thermocouple ( $\pm 0.2$  °C accuracy). Quartz cells with a path length (*l*) of 1.0 cm were used in all instances.

**Preparation of 1 and 3a,b.** An aliquot of **2** dissolved in water was placed in a preweighed 1.5 mL microcentrifuge tube and lyophilized to dryness. The dried powder (15 mg, 11.7  $\mu$ mol) was dissolved in 100  $\mu$ L of dry DMSO and 100  $\mu$ L of a 29  $\mu$ M solution of **4** in DMSO was added followed by 22 equiv (45  $\mu$ L) of diisopropylethylamine (DIEA). The solution was warmed to 40 °C, until HPLC indicated no further reaction (ca. 3 h). Preferential formation of **3a,b** was favored by using fewer equivalents of **2** and shorter reaction times. The solution was diluted to 1.0 mL with 50 mM sodium acetate, pH 6, and purified by sequential ion exchange chromatography (Sephadex CM50; 50 mM sodium acetate, pH 6), reversed phase HPLC (Vydac 1.0 cm C4 peptide/protein column using a gradient of acetonitrile in 10 mM ammonium acetate pH 6.0, 10% to 40% over 40 min at 2.0 mL/min) and size exclusion chromatography (Sephadex G25, fine). FAB-MS of **1**: *m/z* 3145 (MH<sup>+</sup>). FAB-MS of **3a,b**: *m/z* 1882 (MH<sup>+</sup>).

**Preparation of 6.** Peptide **5** (4.0 mg, 2.65  $\mu$ mol) was dissolved in 0.5 mL of H<sub>2</sub>O in a 1.5 mL microcentrifuge tube, and 2 M NaOH was added to pH 10.3 (110  $\mu$ L). Acetic anhydride (110  $\mu$ L, 1.1  $\mu$ mol) was

(16) King, D. S.; Fields, C. G.; Fields, G. B. *Int. J. Peptide Protein Res.* **1990**, *36*, 255–266.

(17) Smith, K. M. *Porphyrins and Metalloporphyrins*; Elsevier: Amsterdam, 1975; p 801.

(18) Collman, J. P.; Denisevich, P.; Konai, Y.; Marrocco, M.; Koval, C.; Anson, F. C. *J. Am. Chem. Soc.* **1980**, *102*, 6027–6036.

then added and the solution stood at room temperature for 5 min, at which time HPLC analysis (and Kaiser ninhydrin test) indicated completion. The product was purified by reverse phase HPLC using the same conditions described for **2**. FAB MS:  $m/z$  1551 ( $MH^+$ ).

**Circular Dichroism Studies.** CD experiments were performed on an AVIV Model 60DS spectrometer at 8 °C, unless otherwise noted. The instrument was calibrated daily using (1S)-(+)-10-camphorsulfonic acid. Temperature control was achieved using a circulating water bath. The actual temperature within the cell was measured using an Omega Model HH200 thermometer with a K thermocouple ( $\pm 0.2$  °C accuracy). For most studies, cell path length ( $l$ ) was 1.0 cm. For the concentration-dependence studies, cell path lengths varied from 0.1 to 10 cm. Spectra in the far UV (190–240 nm) represent the average of 3–5 scans, while those for the Soret band represent the average of 5–10 scans. Spectra in the far UV are reported in terms of mean residue ellipticity ( $[\theta]$ , in  $\text{deg}\cdot\text{cm}^2\cdot\text{dmol}^{-1}$ ), calculated as  $[\theta] = [\theta]_{\text{obs}}(\text{MRW}/10l/c)$  where  $[\theta]_{\text{obs}}$  is the ellipticity measured in millidegrees, MRW is the mean residue molecular weight of the peptide (molecular weight divided by the number of amino acids),  $c$  = sample concentration in mg/mL, and  $l$  = optical path length of the cell in centimeters. Spectra in the Soret region are reported in terms of molar ellipticity ( $[\theta]_m$ , in  $\text{deg}\cdot\text{cm}^2\cdot\text{dmol}^{-1}$ ), calculated as  $[\theta]_m = [\theta]_{\text{obs}}(\text{MW}/10l/c)$  where MW is the molecular weight of the compound.

Stock solutions of each compound in distilled deionized water were prepared and stored in the freezer when not in use. Concentrations of **5** and **6** were determined from the extinction coefficient of indole-3-acetic acid at 275 nm ( $\epsilon = 6100$ ; both measurements were performed in 1:1 ethanol/water). Concentrations of **1** and of **3a,b** in 1:1 ethanol/2.5 M aqueous imidazole were determined using  $\epsilon(403) = 139\,000$  for ferric mesoporphyrin IX chloride (Porphyrin Products, Logan, UT) measured in the same solvent. The error in the measured concentration of both compounds is on the order of  $\pm 10\%$ . Stock solutions were diluted to the appropriate concentration using Gilson pipettes.

## Results and Discussion

**Histidine Environment in Hemoproteins.** Chakrabarti has recently reviewed the literature regarding histidine-metal coordination in proteins.<sup>19</sup> His data show that for proteins in which one or two histidine (His) residues act as ligands to a heme iron, only the  $\epsilon 2$  nitrogen of the imidazolyl group can be involved since severe steric interactions would arise if the  $\delta 1$  nitrogen were employed (Figure 1).

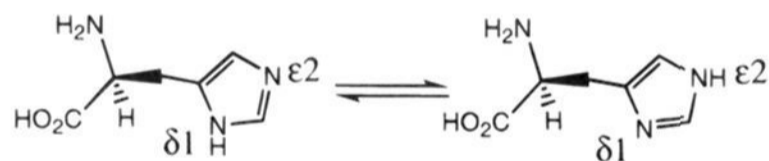


**Figure 1.** The two tautomers of histidine.

When the His residue occurs in a helical region of the protein, the favored angle ( $\angle$ ) between the helix axis and the plane of the heme is determined by the side chain angles adopted by His. Favored amino acid side-chain torsional angles are normally as follows:  $\chi_1 = 60^\circ$  ( $g^-$ ),  $180^\circ$  (t), or  $300^\circ$  ( $g^+$ ). Of the allowed  $\chi_1$  angles,  $g^-$  is highly disfavored for aromatic amino acids, including His. For His residues which occur in  $\alpha$ -helices, the most common  $\chi_2$  values are  $90^\circ$  and  $270^\circ$ . When  $\chi_1 = 300^\circ$  and  $\chi_2 = 90^\circ$ ,  $\angle \approx 0$ , as is observed in hemoproteins such as erythrocyruorin, cytochrome *c*3, hemoglobin, and myoglobin.<sup>19</sup> In addition, with these torsional angles,  $N\delta 1-H$  of His is free to hydrogen bond with the backbone carbonyl of the amino acid at position  $i - 4$ .<sup>19</sup> The angle between the plane of the imidazole ring and a line connecting two opposing nitrogen atoms in the heme is highly variable in bisimidazole coordinated hemes, with an angle of  $45^\circ$  causing minimum steric interactions.<sup>20</sup>

(19) Chakrabarti, P. *Protein Eng.* **1990**, *4*, 57–63.

(20) Collins, D. M.; Countryman, R.; Hoard, J. L. *J. Am. Chem. Soc.* **1972**, *94*, 2066–2072.

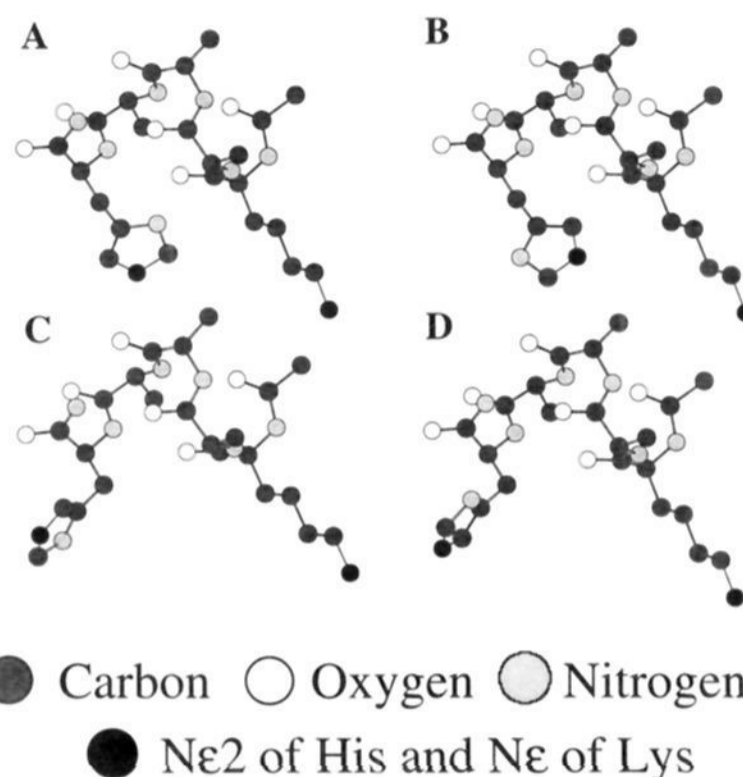


**Figure 2.** Ball and stick figures of the  $\alpha$ -helical peptide Ac-KAAAH-NH<sub>2</sub> with four favorable combinations of histidine side chain torsional angles  $\chi_1$  and  $\chi_2$ . Refer to Table 1 and the text for details.

**Table 1.** Side Chain Torsional Angles ( $\chi_1$  and  $\chi_2$ ) for Histidine<sup>19</sup> in the Five-Residue  $\alpha$ -Helical Peptide Ac-KAAAH-NH<sub>2</sub> (Figure 2) and the Corresponding Distances between N $\epsilon 2$  of Histidine and N $\epsilon$  of Lysine

$\chi_1$ , deg	$\chi_2$ , deg	His(N $\epsilon 2$ )–Lys(N $\epsilon$ ) <sup>a</sup>
300 ( $g^+$ )	90	7.89 Å (A)
300 ( $g^+$ )	270	7.30 Å (B)
180 (t)	90	13.45 Å (C)
180 (t)	270	12.92 Å (D)

<sup>a</sup> A–D refers to the ball and stick structures in Figure 2.

**Design and Synthesis of 1.** Using the Sybyl molecular modeling program,<sup>21</sup> an  $\alpha$ -helical 5-residue peptide having the sequence Ac-KAAAH-NH<sub>2</sub> was created. Several combinations of the  $\chi_1$  and  $\chi_2$  angles discussed above were specified for the His side chain, while the lysine (Lys) side chain was kept in its most extended form ( $\chi_1 = 300^\circ$ ,  $\chi_2 - \chi_4 = 180^\circ$ ). The four His conformations in the model peptides (Figure 2) are among those most commonly encountered for His residues which coordinate to a heme iron from a position within an  $\alpha$ -helical region of a protein.<sup>19</sup> The distance between N $\epsilon$  of Lys and N $\epsilon 2$  of His for each of the conformers in Figure 2 is listed in Table 1. When  $\chi_1 = 300^\circ$  and  $\chi_2 = 90^\circ$  (A in Figure 2), this distance (7.89 Å) most closely approaches the distance between the iron atom and the propionate carboxyl groups of iron mesoporphyrin IX (ca. 8.5 Å). Of the four peptide conformers shown in Figure 2, only A has the Lys and His side chains in the proper orientation to span iron(III) mesoporphyrin IX if the Lys is connected to the heme propionate in an amide linkage and the imidazole is coordinated to the heme iron. As mentioned above, with these His torsional angles, the angle between the helix axis and the plane of the heme will be close to  $0^\circ$ .<sup>19</sup>

We chose to use a helical peptide (**2**) having a length in the range of those found in protein structures (average number of residues/helix = 12),<sup>22</sup> even though a peptide this short would likely not exhibit significant helicity on its own. However, entropic constraints on the peptide backbone imposed by the metal to ligand bonding interaction were expected to cause the amino acids between the attachment points to favor a helical arrangement. In accord with previous research, such binding-induced helix nucleation should favor helix propagation.<sup>7,8</sup>

(21) Sybyl molecular modeling software version 6.01, Tripos Associates, Inc., St. Louis, MO.

(22) Presta, L. G.; Rose, G. D. *Science* **1988**, *240*, 1632–1641.

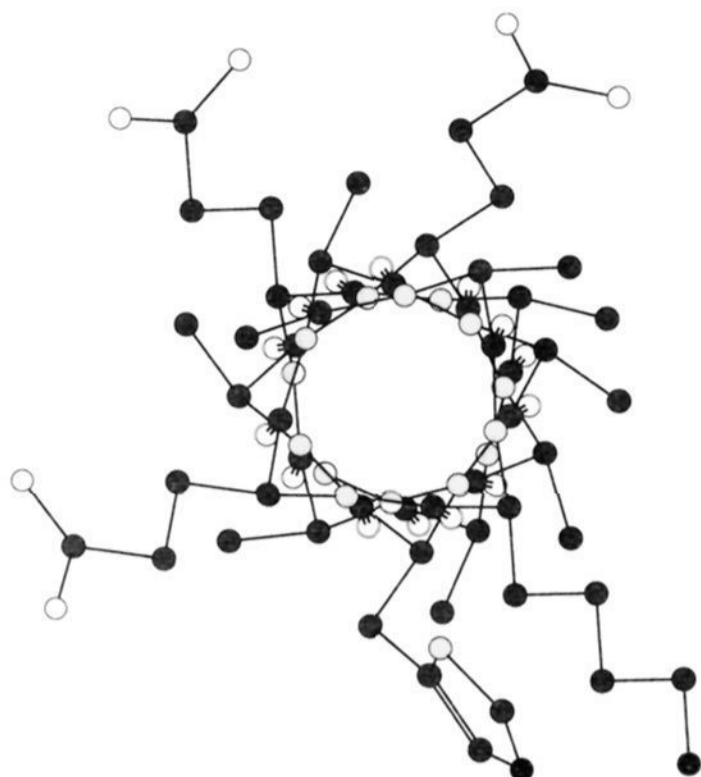


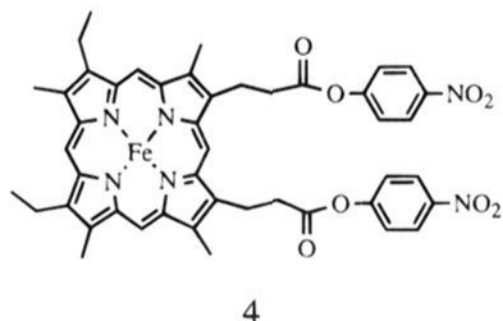
**Figure 3.** Ball and stick figure of peptide **2** in an  $\alpha$ -helical conformation, viewed down the helix axis. The His side chain torsional angles ( $\chi_1$  and  $\chi_2$ ) are identical to those in A, Figure 2.

In order to convey water solubility to the structure, glutamate (Glu) residues were placed in the sequence such that they point away from the heme if the peptide is in an  $\alpha$ -helical conformation (Figure 3). Alanine (Ala) was utilized at all other positions due to its high helical propensity.<sup>1</sup>

Acetylation of the N-terminus and amidation of the C-terminus eliminate repulsive ion-helix dipole interactions and provide two additional hydrogen bonding sites.

Iron(III) mesoporphyrin IX was used instead of the more commonly encountered iron(III) protoporphyrin IX so that side reactions involving the vinyl groups (such as hydration) could be avoided. The substitution pattern of this heme places it in the  $C_2$  symmetry group. If two molecules of **2** are attached to the nonidentical propionate moieties of the heme, the resulting molecule (**1**) has no symmetry ( $C_1$  symmetry group). If the His imidazoles coordinate to the heme iron, two interconvertible diastereomers result. If only one peptide is attached to the propionate groups, two discrete diastereomers should be observed.

Since peptide-sandwiched mesoheme **1** represents a prototype for a general class of synthetic hemoproteins, we desired a simple preparation which would involve a minimum of steps. The Lys  $\epsilon$ -amine was expected to react rapidly and specifically with an activated ester, e.g., the bis-*p*-nitrophenyl ester of iron(III) mesoporphyrin IX (**4**). We thus chose Glu residues to provide water solubility so that we could eliminate deprotection steps. Solubility of **2** in organic solvents is limited, but it does



dissolve in DMSO, as does **4**. Thus, **4** was reacted with four molar equiv of **2** in DMSO containing an excess of diisopropylethylamine, and the solution was warmed to 40 °C until no further increase in the amount of **1** was observed by HPLC (ca. 3 h). Purification was achieved by sequential ion-exchange chromatography (Sephadex CM50), reversed phase HPLC

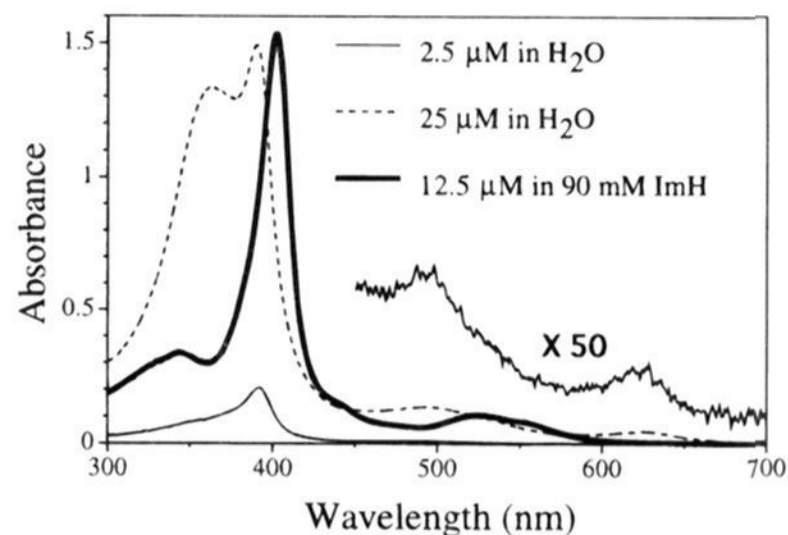


**Figure 4.** UV/vis spectra of **3a,b** in neutral aqueous solution at 2.5  $\mu$ M (—), 25  $\mu$ M (---) and at 12.5  $\mu$ M in 90 mM aqueous imidazole (—) at room temperature. Also shown is the spectrum of the 2.5  $\mu$ M aqueous sample between 450 and 700 nm multiplied by a factor of 50.

(Vydac C4 peptide/protein column) and size exclusion chromatography (Sephadex G-25). A small amount of monopeptide adduct (**3a,b**) was always observed by HPLC, eluting as two broad, poorly resolved peaks. The monopeptide adduct was favored by reducing the number of equivalents of **2** used in the reaction, along with shorter reaction times, and was isolated as a mixture of the two diastereomers.

**UV/vis Spectroscopy.** Visible spectra of **3a,b** at 2.5 and at 25  $\mu$ M concentration in water (Figure 4) and of 7  $\mu$ M iron(III) mesoporphyrin IX in 60/40 H<sub>2</sub>O/EtOH (spectrum not shown) are consistent with the iron(III) in all cases being predominantly high spin.<sup>23</sup> Dominant features in the spectra are the  $\pi$ -iron charge transfer band at 620 nm, the high spin  $\beta$ -band ( $Q_v$ ) at 495 nm, and the Soret band at 391 nm. The most significant difference between the spectra of **3a,b** at 2.5 and at 25  $\mu$ M is the prominent broad band centered near 350 nm in the more concentrated sample. Strikingly similar spectroscopic behavior was reported for the ferriheme octapeptide fragment of cytochrome *c*<sup>14c</sup> and can be attributed to intermolecular heme-heme association. Simple porphyrins are known to aggregate in this concentration range in aqueous solution,<sup>24</sup> and similar properties would be expected for **3a,b** since at least one face of the heme will be solvent-exposed. With 1:1 EtOH/H<sub>2</sub>O as the solvent, the 350 nm band diminishes, while the intensity at 391 nm is increased (data not shown), consistent with the heme-aggregate disrupting properties of ethanol.<sup>24a</sup> In the spectrum of **3a,b** at 25  $\mu$ M concentration, the charge transfer nm band (620 nm) is shifted to slightly longer wavelengths relative to its position in the 2.5  $\mu$ M sample. Enhanced absorbance near 550 nm is also observed in the 25  $\mu$ M sample. Both of these features are consistent with increased intermolecular imidazole-iron coordination at the higher concentration,<sup>25</sup> such that there likely exists some low spin bisimidazole coordinated iron(III) heme in equilibrium with the high spin species.

Visible spectra of high spin iron(III) hemes are not appreciably affected by the nature of the iron coordination sphere. For example, aquomet hemoglobin (one water and one histidine imidazolyl ligand) and the bis-DMSO adduct of iron(III) protoporphyrin IX have visible spectra which are virtually indistinguishable.<sup>26</sup> As a result, using visible spectroscopy we are unable to demonstrate whether intramolecular imidazole to

(23) Adar, F. In *The Porphyrins*; Dolphin, D., Ed.; Academic: New York, 1978; Vol. 3, Chapter 2.

(24) (a) Kolski, G. B.; Plane, R. A. *J. Am. Chem. Soc.* **1972**, *94*, 3740–3744. (b) Pasternack, R. F. *Ann. N. Y. Acad. Sci.* **1973**, *206*, 614–630.

(25) Hasinoff, B. B.; Dunford, B.; Horne, D. G. *Can. J. Chem.* **1969**, *47*, 3225–3232.

(26) Spiro, T. G.; Stong, J. D.; Stein, P. *J. Am. Chem. Soc.* **1979**, *101*, 2648–2655.

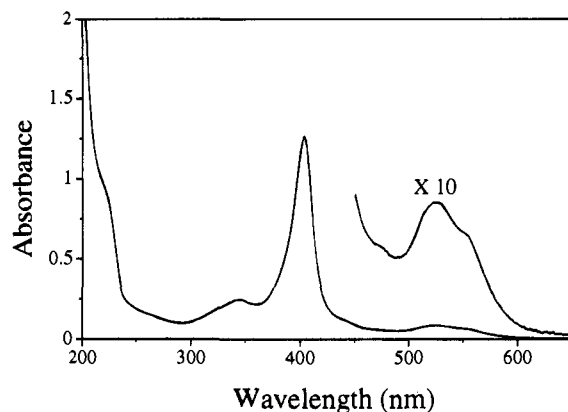


**Figure 5.** UV/vis spectrum of 9  $\mu\text{M}$  **1** in aqueous solution at room temperature. Also shown is the spectrum between 450 nm and 700 nm multiplied by a factor of 10.

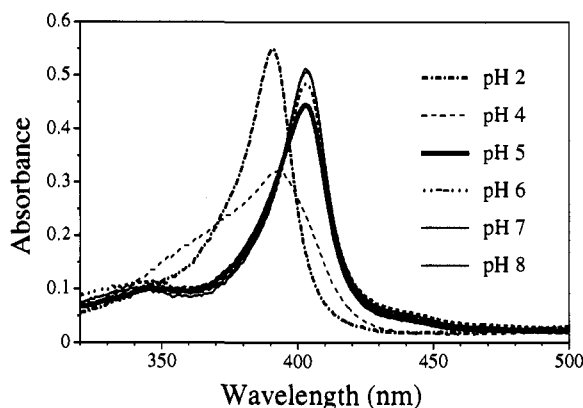


**Figure 6.** UV/vis spectra of the Soret region of **1** (3.5  $\mu\text{M}$ ) between pH 2.0 and 8.0 at room temperature.

iron coordination prevails in **3a,b** at equilibrium. The iron(III) in **3a,b** and in iron(III)mesoporphyrin IX can be converted entirely to the low spin form by addition of exogenous imidazole (loss of the charge transfer and high spin  $\beta$ -bands and enhancement of low spin  $\beta$  ( $Q_v$ ) and  $\alpha$  ( $Q_o$ ) bands at 525 and 565 nm and a shift of the Soret band from 391 to 403 nm; Figure 4).<sup>23</sup> The Soret band in this species is narrow, indicative of a monomeric compound. Urry demonstrated with the ferriheme octapeptide of cytochrome *c* that addition of exogenous imidazole acts to break up heme aggregates in aqueous solution.<sup>14c</sup>

The spectrum of **3a,b** with 90 mM imidazole (Figure 4) is identical to that measured for 8  $\mu\text{M}$  **1** in water (Figure 5), indicating that the desired coordination environment has been achieved in **1**. In marked contrast to **3a,b**, no concentration-dependent changes in optical spectra of **1** are observed between 0.6 and 20  $\mu\text{M}$  at 9  $^\circ\text{C}$ , supporting the CD data in suggesting that **1** exists as a monomer in the concentration range used in our studies (6–10  $\mu\text{M}$ ).<sup>24</sup> No aggregation would be expected for **1**, as bisimidazolyl coordination results in a structure in which both faces of the heme are shielded from the solvent. Optical titration of iron(III) mesoporphyrin IX (5.8  $\mu\text{M}$ ) with imidazole in 60/40  $\text{H}_2\text{O}/\text{EtOH}$  (data not shown) indicated that [imidazole] must be >20 mM (>3000 equiv) to approach saturation binding. This data is consistent with the metal–ligand interactions in **1** being completely intramolecular. The heme coordination is sensitive to solution pH, however, as demonstrated in Figure 6. Between pH 6 and 8, UV/vis spectra of **1** are essentially identical. However, between pH 6 and 4, the spectra change noticeably, with the Soret band shifting toward shorter wavelengths. At pH 2, the Soret band  $\lambda_{\text{max}}$  is at 391 nm (Figure 4), and the charge transfer band at 620 nm and high spin  $\beta$ -band at 495 nm are observed (not shown). Similar pH

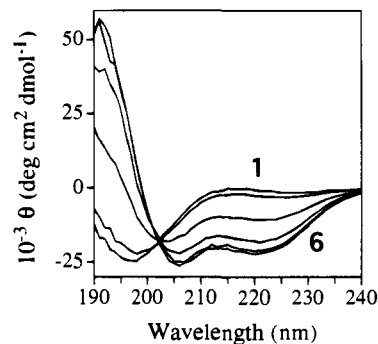


**Figure 7.** CD spectra of peptide **6** (14  $\mu\text{M}$ ) at 8  $^\circ\text{C}$  with increasing volume % of TFE in  $\text{H}_2\text{O}$ . 1: 0%; 2: 10%; 3: 20%; 4: 30%; 5: 40%; 6: 50%.

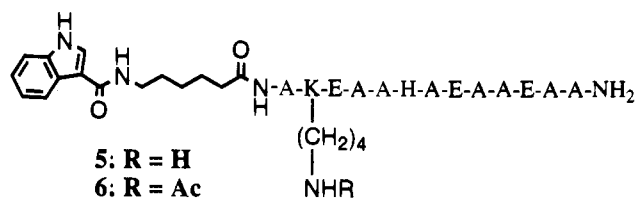
effects are observed for binding of imidazole to simple iron(III) hemes and results from protonation of the His side chain such that it is no longer free to act as a ligand.<sup>24a</sup>

**CD Studies of the Monomeric Peptides.**<sup>27</sup> For a peptide in a helix to coil equilibrium, the fraction of helical peptide ( $f$ ) can be estimated by the mean residue ellipticity in the region of 220–222 nm ( $\theta_{\text{obs}}$ ), as long as the mean residue ellipticity at the appropriate wavelength for the fully helical peptide ( $\theta_{\text{max}}$ ) and for the random coil peptide ( $\theta_0$ ) are known (eq 1).<sup>28</sup> To calculate  $\theta_{\text{max}}$  we use eq 2,<sup>29</sup> where  $n = 13$  and  $\theta_{\infty} = -40\,000$   $\text{deg}\cdot\text{cm}^2\cdot\text{dmol}^{-1}$ , giving  $\theta_{\text{max}} = -27\,700$   $\text{deg}\cdot\text{cm}^2\cdot\text{dmol}^{-1}$ .

$$f = \theta_{\text{obs}} - \theta_0 / (\theta_{\text{max}} - \theta_0) \quad (1)$$

$$\theta_{\text{max}} = \theta_{\infty} [(n - 4)/n] \quad (2)$$

The chromophore-bearing peptide **6** was used for determination of  $\theta_0$  rather than **2** since its concentration could be determined more accurately. Although aromatic amino acids contribute to CD spectra in the far UV region,<sup>30</sup> it has been demonstrated that attaching them to flexible linkers obviates such effects.<sup>31</sup> The extra amide between the 6-aminocaproic acid linker and the indole-3-acetic acid chromophore is not part



of the peptide backbone and therefore was not expected to affect the far UV CD spectrum. The CD spectrum of 14  $\mu\text{M}$  **6** in  $\text{H}_2\text{O}$  at 8  $^\circ\text{C}$  is shown in Figure 7. The dominant CD feature is a strong negative band below 200 nm, indicative of a peptide having a predominantly random coil conformation.<sup>27</sup> A fully helical peptide has the following characteristic CD features: a negative band corresponding to the amide  $n\text{-}\pi^*$  transition in the vicinity of 220–222 nm and a negative band near 208 nm and a strong positive band near 190 nm resulting from exciton coupling of the amide  $\pi\text{-}\pi^*$  transition.<sup>27</sup> When CD spectra of **6** are measured with increasing volume % of the helix-stabilizing solvent 2,2,2-trifluoroethanol (TFE) (Figure 7), a positive band

(27) Woody, R. W. In *The Peptides*; Udenfriend, S., Meienhofer, J., Eds.; Academic: Orlando, FL; Vol. 7, Chapter 2.

(28) Chang, C. T.; Wu, C.-S. C.; Yang, J. T. *Anal. Biochem.* **1978**, *91*, 13–31.

(29) Lyu, P. C.; Sherman, J. C.; Chen, A.; Kallenbach, N. R. *Proc. Natl. Acad. Sci. U.S.A.* **1991**, *88*, 5317–5320.

(30) Manning, M. C. *J. Pharm. Biomed. Anal.* **1989**, *7*, 1103–1119

(31) Chakrabarty, A.; Kortemme, T.; Padmanabhan, S.; Baldwin, R. L. *Biochemistry* **1993**, *32*, 5560–5565.

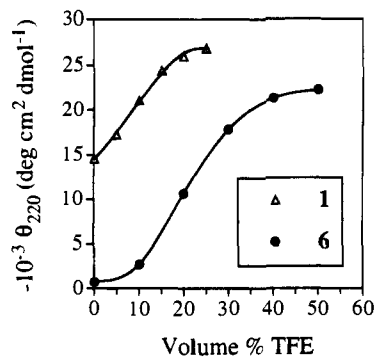


**Figure 8.** Plots of  $\theta_{220}$  vs volume % TFE in  $\text{H}_2\text{O}$  for  $10 \mu\text{M}$  **1** ( $\Delta$ ) and for  $14 \mu\text{M}$  **6** ( $\bullet$ ) at  $8^\circ\text{C}$ .

**Table 2.** CD Data for **1**, **3a,b**, and **6**

compd <sup>a</sup>	solvent <sup>b</sup>	$\theta_{220}$ (deg dm <sup>2</sup> dmol <sup>-1</sup> ) <sup>c</sup>	<i>f</i> (%)
<b>6</b>	60% TFE	-22 000	80
<b>6</b>	60% TFE, pH 2	-26 000	94
<b>6</b>	30% HFIP	-26 000	94
<b>1</b>	100% $\text{H}_2\text{O}$	-14 400	52
<b>1</b>	25% TFE	-26 800	97
<b>3a,b</b> <sup>d</sup>	100% $\text{H}_2\text{O}$	-20 500	74
<b>3a,b</b> <sup>e</sup>	100% $\text{H}_2\text{O}$	-14 700	53

<sup>a</sup> [**6**] =  $14 \mu\text{M}$ ; [**1**] =  $10 \mu\text{M}$ ; temp =  $8^\circ\text{C}$ . <sup>b</sup> Volume % in  $\text{H}_2\text{O}$ . <sup>c</sup>  $\pm 500$  deg dm<sup>2</sup> dmol<sup>-1</sup>; theoretical max = 27 700. <sup>d</sup> [**3a,b**] =  $25 \mu\text{M}$ . <sup>e</sup> [**3a,b**] =  $2.5 \mu\text{M}$ .

emerges at 190 nm, along with two negative bands centered at 206 and at 220 nm. These features are consistent with increasing helical content of the peptides.

A plot of  $\theta_{220}$  vs [TFE] is sigmoidal (Figure 8), signifying that in aqueous solution the peptide has a random coil structure and is not involved in a helix to coil equilibrium.<sup>32</sup> Thus, **6** in aqueous solution is suitable for determining  $\theta_0$  (eq 1), to be used in calculating the helical content of the heme-peptide adducts. The ellipticity at 220 nm in the CD spectrum of **6** in aqueous solution is close to zero. Therefore, a simplified version of eq 1 (eq 3) will be used for determination of peptide helical content. The TFE titration reveals that under strongly helix-inducing conditions (50 volume % TFE), the peptide only

$$f = \theta_{\text{obs}}/\theta_{\text{max}} \quad (3)$$

reaches 80% helical content ( $\theta_{220} = -22\,000 \text{ deg}\cdot\text{cm}^2 \text{ dmol}^{-1}$ ). Acidification of the sample to pH 2 or use of 30 volume % of the more acidic helix-inducing solvent 1,1,1,3,3,3-hexafluoro-2-propanol (HFIP;  $\text{p}K_a = 9.4$ ) results in an additional increase in peptide helicity to approximately 93% (Table 2). Several factors may contribute to limiting the helical propensity of **6** (and of **2**) in TFE under neutral conditions, including the helix-disrupting histidine near the center of the sequence.<sup>6</sup>

**Far-UV CD Studies of 1 and 3a,b.** CD spectra of the monopeptide heme adduct **3a,b** (Figure 9) at  $2.5 \mu\text{M}$  (thin line) and at  $25 \mu\text{M}$  (dashed line) at  $8^\circ\text{C}$  indicate enhanced peptide helicity in this compound relative to **6** in  $\text{H}_2\text{O}$ . However, the CD spectra exhibit concentration-dependent behavior (Figure 9; Table 2). CD features include a positive band near 195 nm and negative bands near 205 and 220 nm. Based on eq 3, a helical content of 53% is calculated for the  $2.5 \mu\text{M}$  sample, nearly identical to that determined for peptide-sandwiched mesoheme **1** (Table 2). However, at the higher concentration the helical content of the peptides (approximately 74% based on eq 3) is significantly increased relative to **1** under identical conditions. Concentration-dependence of the CD spectra for **3a,b** suggests that intermolecular associations lead to alterations

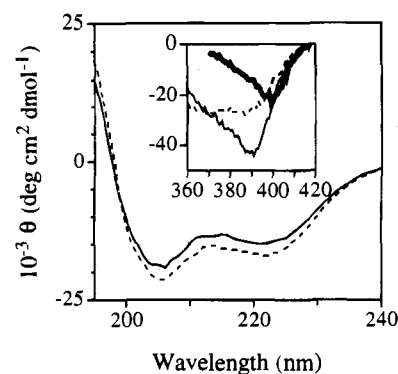


**Figure 9.** Far-UV CD spectra of **3a,b** at  $2.5 \mu\text{M}$  (—) and at  $25 \mu\text{M}$  (---) in  $\text{H}_2\text{O}$  at  $8^\circ\text{C}$ . Inset: CD Soret band of **3a,b** at  $2.5 \mu\text{M}$  (—) in  $\text{H}_2\text{O}$ , at  $25 \mu\text{M}$  in  $\text{H}_2\text{O}$  (---) and in 90 mM aqueous imidazole (—).

in the peptide structure. UV/vis spectroscopy has shown (Figure 4) that heme-heme association and some intermolecular imidazole-iron coordination occurs in **3a,b**. In such an aggregate, peptide-peptide associations are much more likely,<sup>33</sup> which could conceivably account for the concentration-dependent changes observed in CD spectra. The increase in helicity is also consistent with the peptides experiencing a more hydrophobic environment in the aggregated state.

The peptides in **1** exhibit substantially increased helical character relative to **6** at  $10 \mu\text{M}$  concentration in water at  $8^\circ\text{C}$  (maximum near 190 nm, minima near 205 and 220 nm) (Figure 10). The calculated helical content for **1** under these conditions is 52%. In marked contrast to what was observed with **3a,b**, there is no concentration dependence in far-UV CD spectra of **1** between  $0.15 \mu\text{M}$  and  $0.15 \text{ mM}$  (data not shown). Together with the UV/vis studies, these data provide strong evidence that **1** exists as a monomer over a wide range of concentrations. Titration with TFE results in increased intensity of the three major CD bands, along with a shift of the 205 nm band to 207 nm (Figure 10). A plot of  $\theta_{220}$  vs [TFE] is linear at low volume

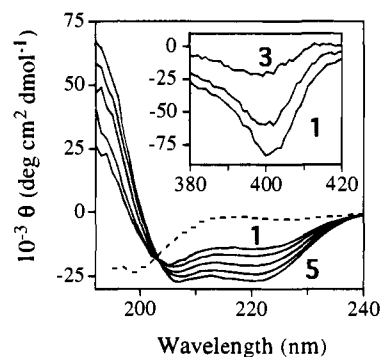


**Figure 10.** Far-UV CD spectra of **1** ( $10 \mu\text{M}$ ) at  $8^\circ\text{C}$  in  $\text{H}_2\text{O}$  at pH = 2 (---) and with increasing volume % TFE in  $\text{H}_2\text{O}$  (1: 0%; 2: 5%; 3: 10%; 4: 15%; 5: 20%). Inset: CD Soret band of **1** at varying volume % TFE in  $\text{H}_2\text{O}$  (1: 0%; 2: 10%; 3: 20%).

% TFE (Figure 8), consistent with **1** being involved in a helix to coil equilibrium in aqueous solution.<sup>32</sup> Maximal helicity ( $f = 97\%$  based on eq 3) is attained between 20 and 25 volume % TFE. However, as discussed in the following section, we have evidence that the heme contributes positive ellipticity in the far-UV region. Therefore, the measured mean residue ellipticity for the peptides in **1** is somewhat smaller than the true value. In contrast to **1**, peptide **6** exists in a completely random coil conformation in aqueous solution. In titrations of **6** with TFE,  $\theta_{220}$  reaches a plateau near 50 volume % (Figure 8). Acidification of an aqueous sample of **1** to pH 2 results in

(32) Jasanoff, A.; Fersht, A. R. *Biochemistry* **1994**, *33*, 2129–2135.

(33) Kaumaya, P. T. P.; Berndt, K. D.; Heidorn, D. B.; Trehwella, J.; Kezdy, F. J.; Goldberg, E. *Biochemistry* **1990**, *29*, 13–23.

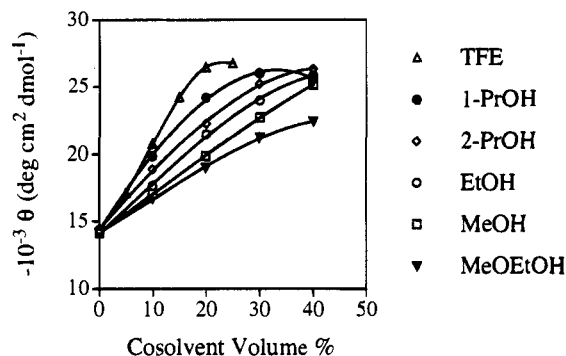


**Figure 11.** Plots of  $\theta_{220}$  vs volume % of several alcohol cosolvents for **1** ( $10 \mu\text{M}$ ) in  $\text{H}_2\text{O}$  at  $8^\circ\text{C}$ .

dissociation of the iron–imidazole bond as demonstrated by UV/vis spectroscopy (Figure 6). Under these conditions, the peptides in **1** exhibit a spectrum consistent with a random coil conformation (negative band below  $200 \text{ nm}$ ; Figure 10, dashed line). This behavior demonstrates that the peptide helicity in **1** results entirely from iron to histidine imidazolyl coordination, as intended in our design.

Alcohols other than TFE, for example, methanol (MeOH), ethanol (EtOH), 1-propanol (1-PrOH), 2-propanol (2-PrOH), and 2-methoxyethanol (MeOEtOH), also influence the structure of peptide-sandwiched mesoheme **1** (spectra not shown). Based on plots of  $\theta_{220}$  vs solvent volume %, the helix-stabilizing ability of these solvents decreases in the following order: TFE > 1-PrOH > 2-PrOH > EtOH > MeOH > MeOEtOH (Figure 11). The relative helix-stabilizing ability of the solvents can be demonstrated by comparing the volume % of each required to increase the helical content of the peptides from 52% to 80% ( $\theta_{220} = -22\,000 \text{ deg}\cdot\text{cm}^2 \text{ dmol}^{-1}$ ). The values are calculated from quadratic equations describing the data in Figure 10 and are as follows: TFE (11.5%), 1-PrOH (14%), 2-PrOH (18.5%), EtOH (22.5%), MeOH (27.6%), and MeOEtOH (36.3%). Note that for the three weakest helix-stabilizing solvents (EtOH, MeOH, and MeOEtOH) helical content of the peptides has not leveled off even at 40 volume % (the highest volume % tested). The most surprising result is that 1-PrOH and 2-PrOH proved to be relatively strong helix-stabilizing solvents for **1** even though they are not normally considered as such. Although 1-PrOH is nearly as effective as TFE at low volume %, it becomes a much weaker helix-stabilizer at higher volume %. We have found no correlation between the helix-stabilizing properties of the six cosolvents listed above and other parameters such as dielectric constant or dipole moment, nor with empirical measures of solvent polarity such as Reichardt's  $E_T(30)$  scale.<sup>34</sup>

**Heme Features in CD Spectra.** A negative band centered at  $390 \text{ nm}$ , corresponding to the Soret band of the heme, is observed in CD spectra of the monopeptide adduct **3a,b** (Figure 9, inset). The CD Soret band of **3a,b** is strongly concentration-dependent, which mirrors its behavior in UV/vis spectra (compare Figure 4). The band is considerably sharper at the lower concentration. Addition of imidazole ( $90 \text{ mM}$ ) to the  $25 \mu\text{M}$  sample of **3a,b** results in a shift of the CD Soret band to approximately  $400 \text{ nm}$  (Figure 9, inset; bold line) with concomitant sharpening, once again mirroring the effects observed in optical spectra (Figure 4). Sharpening of the CD Soret band in the heme–peptide adducts of cytochrome *c* has also been previously observed upon heating and by addition of exogenous imidazole, conditions which act to break up aggregation.<sup>14c</sup> Unfortunately, it is not possible to investigate the effects of imidazole binding on the far-UV CD of **3a,b**, as imidazole absorbs too strongly in this region.

(34) Reichardt, C. *Solvents and Solvent Effects in Organic Chemistry*, 2nd ed.; VCH: Weinheim, 1990; Chapter 7.

CD features attributable to the heme are also observed in the peptide-sandwiched mesoheme **1**, including a negative Soret band at  $403 \text{ nm}$  ( $\theta_{m403} = -82\,000 \text{ deg}\cdot\text{cm}^2 \text{ dmol}^{-1}$ ; Figure 10, inset) and the  $\alpha$  and  $\beta$  bands between  $500$  and  $600 \text{ nm}$  (spectrum not shown). Since the heme ring is achiral, the CD features in both **1** and **3a,b** must be induced by the peptide component of the molecule. Consistent with this, when the iron–imidazole bonds of **1** are dissociated by reducing the solution pH to 2, the CD Soret band vanishes (spectrum not shown). As with the far-UV CD spectrum, the Soret band spectrum is concentration-independent between  $0.3 \mu\text{M}$  and  $0.15 \text{ mM}$ , further supporting the notion that peptide-sandwiched mesoheme **1** exists as a monomer in the range of concentrations employed in the UV/vis- and CD studies.

In other heme–peptide adducts,<sup>13</sup> and in natural hemoproteins,<sup>14</sup> CD bands arising from the heme are often observed, their shapes, magnitude, and sign (i.e., positive or negative Cotton effect) depending on the protein environment surrounding the heme, and the oxidation state and coordination sphere of the heme iron. In the absence of a chiral appendage or a protein framework, the heme is achiral, and thus has no CD features. The heme Soret absorption band arises from two nearly degenerate electronic transitions ( $B_x$  and  $B_y$ ) which are polarized perpendicularly to each other and which are of opposite sign.<sup>35</sup> When the heme is in an asymmetric environment, as in **1**, subtle changes can alter the relative intensities of  $B_x$  and  $B_y$  as well as their orientation with respect to the heme framework. For example, the CD Soret band of leghemoglobin is converted from negative to positive ellipticity simply by coordination of various ligands on the distal side of the heme.<sup>36</sup> According to Hsu and Woody,<sup>37</sup> coupled oscillator interactions between  $B_x$  and  $B_y$  and  $\pi$ – $\pi^*$  transitions of aromatic amino acids such as tyrosine, tryptophan, and histidine are the primary contributors to the CD Soret band in hemoproteins. Their calculations indicate that neither the peptide backbone amides, nonaromatic amino acid side chains, nor the proximal imidazole (analogous to the imidazole ligands in **1** and **3a,b**) are significant contributors to the CD Soret band in hemoproteins. However, CD Soret and  $\alpha$  and  $\beta$  bands have been observed in a number of heme–peptide adducts, most notably fragments resulting from enzymatic digestion of cytochrome *c* (the microperoxidases), which contain no aromatic amino acids other than the histidine residue which acts as the ligand to the heme iron in the native protein.<sup>14</sup> Rather than resulting from coupling of the  $B_x$  and  $B_y$  transitions of the heme with nearby chromophores, it has been postulated that in the microperoxidases heme CD features arise via a lowering of the symmetry of the heme group due to differences in the ligand field strength of the two axial ligands.<sup>35a,b</sup> A similar phenomenon could possibly explain the CD features of monopeptide adduct **3a,b** in aqueous solution, although it would not be appropriate for peptide-sandwiched mesoheme **1** for which both ligands to the iron are identical nor for **3a,b** in  $90 \text{ mM}$  imidazole (the ligand field strengths of imidazole and of the His imidazolyl side chain should be nearly identical). A system with an interesting analogy to **1** is the noncovalent complex between poly-L-lysine and iron(III) protoporphyrin IX, originally reported by Blauer.<sup>38</sup> At pH 12, poly-L-lysine is predominantly  $\alpha$ -helical, and a strong negative Soret band is

(35) Reviewed in: (a) Myer, Y. P.; Pande, A. In *The Porphyrins*; Dolphin, D., Ed.; Academic: New York, 1978; Volume 3, Chapter 6. (b) Myer, Y. P. *Methods Enzymol.* **1978**, *54*, 249–284. (c) Hatano, M. *Adv. Polym. Sci.* **1986**, *77*, 1–135.

(36) Lampe, J.; Rein, H.; Scheler, W. *FEBS Lett.* **1972**, *23*, 282–284. (37) Hsu, M.-C.; Woody, R. W. *J. Am. Chem. Soc.* **1971**, *93*, 3515–3525.

(38) (a) Blauer, G. *Nature (London)* **1961**, *189*, 396. (b) Blauer, G. *Biochim. Biophys. Acta* **1967**, *79*, 547.

(39) Tsuchida, E.; Hasegawa, E.; Honda, K. *Biochim. Biophys. Acta* **1976**, *427*, 520–529.

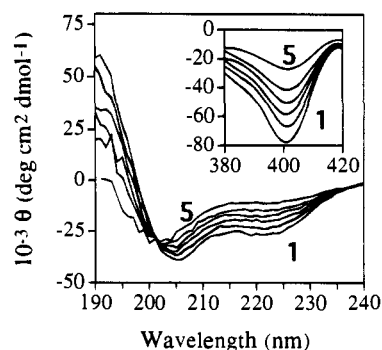


**Figure 12.** Far-UV CD spectra and Soret band CD spectra (inset) of **1** ( $8 \mu\text{M}$ ) in  $\text{H}_2\text{O}$  measured at the following temperatures: 1:  $8.0^\circ\text{C}$ ; 2:  $15.6^\circ\text{C}$ ; 3:  $25.2^\circ\text{C}$ ; 4:  $34.7^\circ\text{C}$ ; 5:  $44.2^\circ\text{C}$ ; 6:  $55.7^\circ\text{C}$ .

observed in CD spectra of the heme complex.<sup>39</sup> The heme iron is low spin, indicating that two lysine side chain amines act as ligands. Therefore, the heme CD features likely do not arise as a result of unsymmetrical ligation of the heme iron. Rather, it has been suggested that they arise via interaction between the  $B_x$  and  $B_y$  transition dipoles in the heme with the peptide backbone amides, or by induction of dissymmetry (nonplanarity) in the heme ring.<sup>35a,b</sup>

When the helical content of **1** is increased by titration with increasing volume % of TFE, the CD Soret band diminishes, reaching a minimum molar ellipticity of approximately  $-15\,000 \text{ deg}\cdot\text{cm}^2 \text{ dmol}^{-1}$  (Figure 10, inset). It also undergoes a slight hypsochromic shift (to approximately 399 nm) as is observed in UV/vis spectra (data not shown) under the same conditions. Similar reduction in the intensity of the CD Soret band is observed with increasing volume % of 1-PrOH, 2-PrOH, MeOH, EtOH, and MeOEtOH (data not shown). As the fraction of peptide random structure is decreased by addition of helix-stabilizing cosolvents, there should result a greater alignment (ordering) of the peptide backbone amides. Increased alignment would alter the average orientation of the transition dipoles of the amides relative to the  $B_x$  and  $B_y$  transitions of the heme. Such an ordering could, in part, explain the observed diminution of the CD Soret band. Other potential arguments for explaining this phenomenon include (1) a change in the orientation of the His imidazolyl ligands relative to the heme, (2) reduced physical contact between the peptide backbone amides and the heme, or (3) decreasing dissymmetry (distortion) of the heme ring. A combination of these effects is also a possibility. Partial dissociation of the imidazole-iron bonds cannot explain the reduced CD Soret band, as UV/vis spectroscopy indicates that the heme coordination sphere is not altered in the presence of cosolvents nor at elevated temperatures.

Raising the temperature of an aqueous sample of peptide-sandwiched mesoheme **1** results in an expected decrease in peptide helicity (e.g., increased random structure) as determined by a temperature-dependent drop in  $\theta_{220}$  (Figure 12). A corresponding decrease in the intensity of the CD Soret band is also observed (Figure 12, inset). Based on the solvent studies with **1**, it might be expected that temperature-dependent loss of peptide helicity should result in *enhanced* intensity of the CD Soret band. However, we hypothesize that at lower temperatures there is extensive intramolecular contact between the peptide and the heme ring, which is driven by hydrophobic forces (exclusion of solvent water). The kinetic energy acquired by the peptides at higher temperatures will counterbalance the hydrophobic forces, and the average distance between the heme and the peptides will increase. Therefore, one would expect CD features induced by the amides to become less prominent, as observed. If the backbone amides are a major source of the heme CD features, as the cosolvent and thermal data suggest,

then both distance *and* orientation of the amides relative to the heme will be important factors. The conformation of the histidine residues will be largely determined by the metal-to-ligand bond and by the enhanced helical character of the amino acids between it and the lysine residue which anchor the peptide to the heme.<sup>19</sup> Therefore, it is not likely that a small increase in peptide helical content would result in significant reorientation of the imidazolyl side chain, as would be required for the large observed changes in the CD Soret band. Regardless, neither imidazole orientation nor heme distortion can be discounted as additional potential sources of heme optical activity.

It has been documented that the CD Soret bands of various hemoproteins undergo time-dependent changes after reconstitution of the apoprotein with heme (increasing intensity over a period of hours to days).<sup>40</sup> It is believed that the observed alteration results from a change in the equilibrium distribution of heme orientations within the heme pocket, consistent with prior  $^1\text{H}$  NMR findings.<sup>41</sup> In the two conformations, the  $B_x$  and  $B_y$  electronic transitions of the heme will have opposite orientations with respect to the surrounding protein chromophores. Thus it was postulated<sup>40b,e</sup> that for the "wrong" heme orientation (which is more heavily populated upon initial reconstitution of the holoprotein than at equilibrium), coupling between the heme  $B_x$  and  $B_y$  transitions and various transitions of nearby chromophores will be opposite to those for the "right" heme orientation. For this mechanism, the innate CD Soret band for the "wrong" conformation is assumed to be negative, while that for the "right" conformation is positive, such that decreasing negative contribution to the CD Soret band occurs over time. However, heme-protein interactions will also be dissimilar for the two heme orientations owing to unequal steric requirements.<sup>40a</sup> Santucci et al.<sup>40a</sup> and Light et al.<sup>40c</sup> have postulated that the reduced CD Soret band for the "wrong" conformation arises simply as a result of weaker heme-protein contact (e.g., greater average distance between the heme ring and the surrounding protein structure). If this mechanism for time-dependent increase of Soret band intensity is correct, the Cotton effects of the CD Soret bands need not be of opposite sign for the two different orientations. Our results are consistent with the second mechanism. We observe changes in the CD Soret band of **1** by manipulation of the peptide structure, rather than as a function of time. Solvent and temperature studies of **1** have shown that minor alterations of peptide conformation in the vicinity of a heme strongly influence heme optical activity. One would expect that the perturbations of myoglobin structure produced by binding of heme in the "wrong" orientation would likewise be relatively minor. Interestingly, the increase in intensity of the CD Soret band recorded for **1** with decreasing peptide helical content is of similar magnitude to the increased intensity of the CD Soret band of reconstituted myoglobin recorded as a function of time. Recently it was reported that for complexes formed between zinc porphyrins and amino acid esters, heme CD Soret bands arise via coupling of the heme  $B_x$  and  $B_y$  transitions with electronic and magnetic transitions of the ester.<sup>15</sup> This finding further supports our contention that the peptide backbone amides are the major source of the heme CD features for both **1** and **3a,b**.

(40) (a) Santucci, R.; Ascoli, F.; La Mar, G. N.; Pandey, R. K.; Smith, K. M. *Bioch. Biophys. Acta* **1993**, *1164*, 133–137. (b) Santucci, R.; Mintorovitch, J.; Constantinidis, I.; Satterlee, J. D.; Ascoli, F. *Biochem. Biophys. Acta* **1988**, *953*, 201–204. (c) Light, R. W.; Rohlfs, R. J.; Palmer, G.; Olson, J. S. *J. Biol. Chem.* **1987**, *262*, 46–52. (d) Bellelli, A.; Foon, R.; Ascoli, F.; Brunori, M. *Biochem. J.* **1987**, *246*, 787–789. (e) Aojula, H. S.; Wilson, M. T.; Drake, A. *Biochem. J.* **1986**, *237*, 613–616.

(41) (a) La Mar, G. M.; Smith, W. S.; Davis, N. L.; Budd, D. L.; Levy, M. J. *Biochem. Biophys. Res. Commun.* **1989**, *158*, 462–468. (b) Yamamoto, Y.; La Mar, G. N. *Biochemistry* **1986**, *25*, 5288–5297.



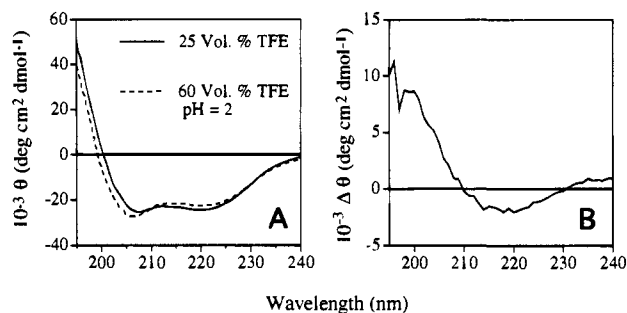


**Figure 13.** (a) CD spectra of **1** (9 μM) in 25 volume % TFE (—) and in 60 volume % TFE, pH 2 (---). (b) Difference spectrum obtained by subtracting the 25 volume % spectrum from the 60 volume % spectrum.

Contribution of aromatic amino acids to far-UV CD spectra of polypeptides has been well-documented,<sup>27,30</sup> and can result in misinterpretation of peptide secondary structure analysis if not accounted for.<sup>31</sup> Whether the aromatic chromophore contributes positive or negative ellipticity in this region depends on the nature of the interaction between its electronic transitions and the transition dipoles within the aromatic group.<sup>31</sup> Heme groups are also known to contribute to the far-UV CD of hemoproteins.<sup>13</sup> For example, X-ray crystallographic studies have shown that myoglobin<sup>42</sup> and leghemoglobin<sup>43</sup> have similar helical contents, but their far-UV CD spectra are significantly different.<sup>13a</sup> Nicola et al. concluded that in the case of leghemoglobin, optical activity of the heme (positive ellipticity) subtracts from the intrinsic far-UV CD spectrum of the protein, resulting in an underestimate of protein helical content.<sup>13a</sup> In contrast, there is an apparent additive effect with myoglobin. Our investigations of **1** have suggested that the heme contributes to far-UV CD spectra, although it is presently not possible to quantify the extent of the effect. The heme contribution can be most readily observed if one compares spectra of **1** under conditions of maximum peptide helical content with the iron-imidazole bonds intact (25 volume % TFE) and with the iron-imidazole bonds dissociated (60 volume % TFE, pH 2) (Figure 13a). This is done rather than comparing **1** with **6** in order to guarantee equal concentration of the peptide under the two sets of conditions. A difference spectrum is shown in Figure 13b. From  $\theta_{220}$  it can be determined that the helical content is greater for the peptide when the histidines are coordinated to the heme iron (Figure 13a, solid line). However, for the complexed structure, reduced ellipticity relative to the noncoordinated compound is observed at wavelengths shorter than 210 nm and longer than 231 nm. Normally, one expects increased intensity in both of these regions of the spectrum as peptide helicity is increased (compare Figures 7 and 10). The isodichroic point in TFE titrations of **1** and of **6** is at approximately 203 nm (Figures 7 and 10). If under these two sets of conditions the peptides were merely at different points within a helix to coil equilibrium, the difference spectrum should cross zero at 203 nm rather than at 210 nm. Likewise, the spectra would be expected to converge between 240 and 250 nm rather than crossing at 231 nm as is observed in the present case. These data suggest that the heme contributes positive ellipticity throughout the entire far-UV range. If this is the case, values of  $f$  calculated from eq 3 represent an *underestimate* of the actual peptide helical content in **1**. As can be seen in the UV/vis spectrum of **1** (Figure 5), the heme absorbs strongly between 240 and 190 nm. Since the heme Soret and  $\alpha$  and  $\beta$  bands are observed in CD spectra, it is reasonable to expect that bands in the far UV region will appear as well. However, we cannot

discount the possibility that under the two sets of conditions there exist differences in the distribution of peptide secondary structure (e.g.,  $\alpha$ -helix,  $\beta$ -strand, turn, and random coil components) which could account for the differences in the CD spectra in Figure 13. For example, enhanced ellipticity at 208 nm for the peptides when detached from the heme iron (Figure 13a, dashed line) could represent increased contribution of  $\beta$ -turns to the average peptide structure relative to the structure with coordinated peptides (Figure 13a, solid line). The most reasonable possibility is that the observed differences in CD spectra as seen in Figure 13 are due to a combination of the two effects. The fact that the CD Soret band of **1** is sensitive to peptide conformation suggests the possibility that the far-UV CD features will be as well. The nature of the heme contribution to the far-UV CD is the subject of ongoing research in our lab.

## Conclusions

We have prepared a water-soluble synthetic hemoprotein (**1**) in which two short covalently attached peptides coordinate to the heme iron via histidine side chains. The peptides in **1** have approximately 52% helical content in aqueous solution as determined by CD, in contrast to the monomeric peptide **6** which exists exclusively in a random coil conformation. The heme in **1** also exhibits CD features, including the Soret band at 403 nm and the  $\alpha$  and  $\beta$ -bands between 500 and 600 nm. Dissociation of the iron-imidazole bond by addition of HCl yields a CD spectrum consistent with a random coil conformation and also results in disappearance of the heme CD features, consistent with both the peptide helicity and the heme CD features arising as a result of iron to imidazole coordination. We also have evidence that the heme contributes significantly to the CD spectrum in the far-UV region, rendering quantitation of actual peptide helicity difficult. The helical content of the peptides can be enhanced by the addition of various alcohol co-solvents, which also results in decrease in the intensity of the CD Soret band. In tandem with the effect of increased temperature on the CD spectra of **1**, the solvent studies suggest that the intensity of the CD Soret band is a function of intramolecular heme-peptide interactions. The most important interactions likely are distance and orientation of the peptide backbone amide transition dipoles relative to the heme  $B_x$  and  $B_y$  transition dipoles. The structural flexibility of **1** will allow a more thorough investigation of the factors responsible for heme features in CD spectra than has previously been possible with hemoproteins or hemoprotein model compounds. Our current efforts are directed toward a more thorough analysis of the effect of co-solvents (including nonalcoholic solvents) on the structure of **1** as well as preparation of variants in which we may investigate the effect of the helix dipole and of designed hydrophobic interactions on peptide helicity. We have also commenced a <sup>1</sup>H NMR study on the diamagnetic iron(II) derivative of **1** and of related compounds and will report our progress in due course.

**Acknowledgment.** This material is based upon work supported by the National Science Foundation under EPSCoR Grant No. OSR-9255223. The Government has certain rights in this material. This work also received matching support from the State of Kansas. Start-up support from The University of Kansas College of Liberal Arts and Sciences is gratefully acknowledged. B.R.H. acknowledges summer support from the NSF Research Experience for Undergraduates (REU) program. FAB MS measurements were performed by the KU Mass Spectrometry Facility.

(42) Phillips, S. E. *V. J. Mol. Biol.* **1980**, *142*, 531–554.

(43) Arutyunyan, E. G.; Kuranova, I. P.; Vainshtein, B. K.; Steigemann, W. *Sov. Phys. Crystallogr.* **1980**, *25*, 43–58.